Journal of Hazardous Materials 180 (2010) 274–281

Contents lists available at ScienceDirect

Journal of Hazardous Materials

journal homepage: www.elsevier.com/locate/jhazmat

Enhancement of the bentonite sorption properties

Annamária Mockovčiaková [a,*], Zuzana Orolínová [a], Jiří Škvarla [b]

[a] Institute of Geotechnics, Slovak Academy of Sciences Watsonova 45, 04354 Košice, Slovakia
[b] Institute of Montaneous Sciences and Environmental Protection, Technical University in Košice, Park Komenského 19, 04200 Košice, Slovakia

ARTICLE INFO

Article history:
Received 6 October 2009
Received in revised form 6 February 2010
Accepted 8 April 2010
Available online 14 April 2010

Keywords:
Montmorillonite
Magnetic composite
Structural
Surface and pore properties
Sorption
Low concentration

ABSTRACT

The almost monomineral fraction of bentonite rock–montmorillonite was modified by magnetic particles to enhance its sorption properties. The method of clay modification consists in the precipitation of magnetic nanoparticles, often used in preparing of ferrofluids, on the surface of clay. The influence of the synthesis temperature (20 and 85 °C) and the weight ratio of bentonite/iron oxides (1:1 and 5:1) on the composite materials properties were investigated. The obtained materials were characterized by the X-ray diffraction method and Mössbauer spectroscopy. Changes in the surface and pore properties of the magnetic composites were studied by the low nitrogen adsorption method and the electrokinetic measurements. The natural bentonite and magnetic composites were used in sorption experiments. The sorption of toxic metals (zinc, cadmium and nickel) from the model solutions was well described by the linearized Langmuir and Freundlich sorption model. The results show that the magnetic bentonite is better sorbent than the unmodified bentonite if the initial concentration of studied metals is very low.

1. Introduction

The heavy metal pollution occurs in many industrial wastewaters, contaminating the surrounding soils. Therefore looking for the most available wastewater treatment is of great interest. The natural clays, being comprised of mixtures of fine grained crystals of clay and other minerals (including metal oxides) play an important role in the environment by taking up cations and anions through adsorption or ion exchange. Using them as adsorbents of metal ions received wide attention because of their easy availability and comparatively less cost [1]. Clays containing montmorillonite are referred to as bentonite, which belongs in the 2:1 clay family, composed of two tetrahedrally coordinated sheets of silicon surrounding an octahedrally coordinated sheet of aluminium ions. An evaluation of the montmorillonite sorption properties for the removal of heavy metals Ni and Cu was made in [2].

Clays can be modified to improve their sorption ability [3,4]. The sorption of toxic metals As, Cd, Cr, Co, Cu, Fe, Pb, Mn, Ni and Zn on natural and modified kaolinite and montmorillonite was described in [5], where the modification of clays was carried out by pillaring and acid activation. The adsorption of zinc from water solutions on the natural and Na-enriched bentonite was studied in [6]. The removal of copper on manganese oxide coated bentonite was studied in [7]. Another kind of clay modification is the magnetic modification, when, for example, the bentonite is coated with iron oxides [8]. The term iron oxides is often used in the scientific literature to describe the group of iron compounds with hydroxide, oxyhydroxide and oxide structures. They are widely put into practice as pigments, catalysts, sorbents, in ferrofluids [9], etc. and the route of chemical synthesis has a significant influence on their chemical, structural and physical properties. The montmorillonite supported magnetite nanoparticles prepared by co-precipitation [10] were studied for the Cr(VI) removal. It seems to be useful to combine sorption properties with magnetic properties to produce novel kinds of magnetic sorbents. In [11], the magnetic sorbent was used for the removal of humic acid. Another, a very attractive application of the modified bentonite was published by authors [12], offering for MRI diagnostics of the gastrointestinal tract a very cheap oral contrast agent for imaging.

In this study the low cost sorbent—natural bentonite was modified by precipitation of iron oxides in order to obtain sorbent with better sorption properties. The changes in surface properties of new composites were studied by the nitrogen adsorption and electrokinetic measurements, the morphology of the composite by TEM measurements. Changes in the structural properties were determined by XRD and Mössbauer spectroscopy measurements. The sorption propensity of the selected composites was verified for removal of zinc, cadmium and nickel from model aqueous solutions.

2. Materials and methods

2.1. Materials

The natural bentonite from the deposit Stará Kremnička (Slovakia), with the formula $[Si_{7.95}\ Al_{0.05}]\ [Al_{3.03}\ Fe_{0.22}\ Mg_{0.75}]\ O_{20}$

* Corresponding author. Tel.: +421 55 7922612, fax: +421 55 7922604.
E-mail address: mocka@saske.sk (A. Mockovčiaková).

0304-3894/$ – see front matter © 2010 Elsevier B.V. All rights reserved.
doi:10.1016/j.jhazmat.2010.04.027

Nomenclature

S_{BET}	specific surface area [m^2/g]
p/p_0	relative pressure
V_{micro}	micropore volume [cm^3/g]
S_t	external surface [m^2/g]
V_a	total pore volume [cm^3/g]
ζ	zeta potential [mV]
C_0	initial metal ion concentration [mg/l]
C_e	equilibrium metal ion concentration in a solution [mg/l]
q_e	amount of metals adsorbed at equilibrium [mg/g]
Q_m	monolayer capacity [mg/g]
K	Langmuir constant [l/mg]
K_f	Freundlich constant related to sorption capacity [l/g]
n	Freundlich constant related to sorption intensity
R^2	coefficient of determination

$(OH)_4$ ($Ca_{0.42}Mg_{0.04}Na_{0.01}K_{0.01}$) was used in this study. The bentonite was at first treated by sedimentation method [13], after that an almost monomineral fraction of montmorillonite (>80%) with the particle size below 20 μm was obtained. The magnetic bentonite was prepared in the solution containing the mixture of iron ions ($FeSO_4{\cdot}7H_2O$ and $FeCl_3$ salts with a ratio of Fe^{3+}:Fe^{2+} = 2:1), where the pretreated bentonite (montmorillonite) was added. After dropping NH_4OH in the solution during a continuous 30 min stirring in nitrogen atmosphere at two temperatures (ambient and 85 °C), the iron oxide particles were precipitated on the surface of bentonite. The final product was washed with the de-ionized water to remove the unfixed iron oxide particles and dried at the temperature of 70 °C. Changing the bentonite/iron oxide weight ratios from 1:1 to 5:1, various composite magnetic materials were obtained. Two of them, denoted as A and E (corresponding to the limiting ratios 1:1 and 5:1), were chosen for this study.

2.2. XRD measurements

XRD qualitative analyses were performed with a Philips PW1820 diffractometer (Germany) equipped with a Cu Kα radiation (40 kV, 40 mA). The iron oxides phases were identified using the JCPDS PDF database

2.3. Mössbauer spectroscopy measurements

Mössbauer spectroscopy measurements were carried out with a 57Co/Rh-ray source at the room temperature. The velocity scale was calibrated relative to 57Fe in Rh. The recoil spectral analysis software was used for the quantitative evaluation of the Mössbauer spectra [14].

2.4. Transmission electron microscopy (TEM) measurements

The size, shape and the arrangement of the particles comprising the sample A85 were investigated by the field emission transmission electron microscopy FE-TEM, JEOL JEM-2100F.

2.5. Nitrogen adsorption experiments

The surface and pore properties of prepared bentonite/iron oxide composites (A20, A85, E20, E85) were characterized by the nitrogen adsorption measurements realized at 77 K with the ASAP 2400 sorption apparatus (Micrometrics). The specific surface area S_{BET} was calculated from the adsorption isotherms according to the BET (Brunauer, Emmett and Teller) method in a range of relative pressure 0.03–0.2 p/p_0. The value of total pore volume V_a was obtained from the maximum adsorption at the relative pressure 0.99 p/p_0. The micropore volume V_{micro} as well as the value of external surface S_t was obtained from the *t*-plot analysis. The pore size distribution of studied samples was calculated from desorption isotherms using the BJH (Barett–Joyner–Halenda) method.

Table 1
Structural parameters of natural bentonite and its composites.

Sample	S_{BET} [m^2/g]	V_a [cm^3/g]	V_{micro} [cm^3/g]	S_t [m^2/g]
Bentonite	39.4	0.096	0.005	27.6
Composite A20	73.7	0.216	0.004	64.2
Composite E20	90.7	0.187	0.002	83.9
Composite A85	82.8	0.251	0.004	73.7
Composite E85	84.8	0.183	0.003	77.5

2.6. Electrokinetic measurements

The surface charge of natural and modified bentonite as well as of the synthesized iron oxides in distilled water was evaluated as a function of pH by using the laser-Doppler electrophoretic light scattering (ZetaPlus, Brookhaven Instruments, USA). To modify the pH of the dispersions, concentrated NaOH and HCl solutions were added in water dropwise. The measured ELS spectra were analysed and electrophoretic mobilities of the dominant peaks were converted into zeta (ζ) potentials according to the Smoluchowski formula (i.e. without any other corrections). This is applicable for relatively coarse particles of bentonite whose size (of faces) exceeds their double-layer thickness (inverted Debye length). However, the nanometric iron oxide particles were also expected to be of the same concern due to their spontaneous agglomeration (no special care was taken to prevent it). The same is true for the bentonite/iron oxide composites.

2.7. Batch sorption experiments

The sorption of zinc, cadmium and nickel on natural bentonite, composite E20 and A85 was conducted at 20 °C in 50 ml capped tubes placed on a rotary shaker for 24 h in order to attain the equilibrium. The reaction mixture consisted of a total 15 ml, containing 2 g/l sorbent material and the desired concentration of metals ranging from 10 to 750 mg/l. The amount of sorbents for cadmium sorption was 1 g. The solution pH was adjusted with 0.01 M HNO_3 and 0.01 M NaOH to the value 5, resulting from the sorption experiments realized at different pH. After the period of 24 h, the supernatant was removed by filtration. The final metal concentration was determined by the atomic absorption spectroscopy (AAS using a Varian 240 RS/2400). The metal uptake was calculated from the difference between the initial and final concentrations of the metal. The sorption isotherms for zinc, cadmium and nickel were fitted with the linearized Langmuir and Freundlich equation.

3. Results and discussion

3.1. Adsorption measurements

The nitrogen adsorption/desorption isotherms of the natural and modified bentonite are shown in Figs. 1 and 2. Apparently, their characteristic features, i.e. the hysteresis loops are associated with the capillary condensation in mesopores. The rising final parts of the isotherms show an occurrence of macropores in the pore structures of studied samples [15]. Table 1 summarizes the values of BET surface area, external surface and the total pore volume. The higher values of specific surface area and the increased values

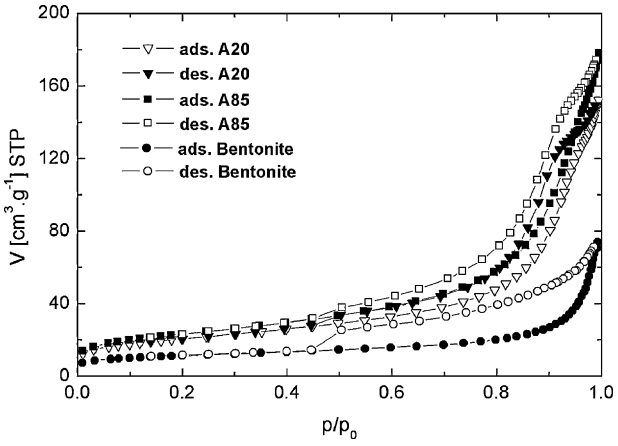

Fig. 1. N_2 adsorption/desorption isotherms of bentonite and composite A.

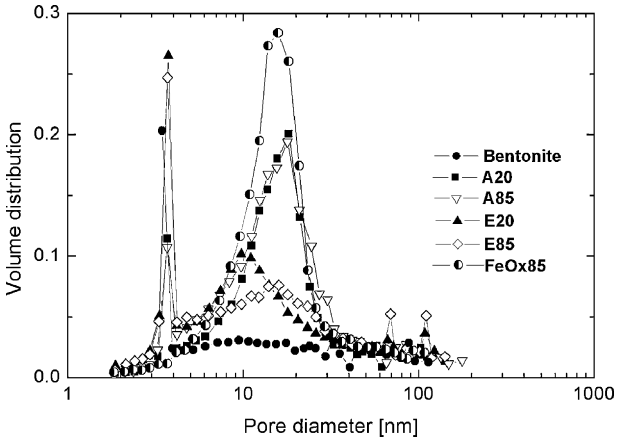

Fig. 3. Pore size distribution of investigated samples.

of total pore volume are related to the agglomerated structure of iron oxides particles created on the surface of bentonite during the precipitation process. As it is seen from the adsorption and desorption isotherms of synthetized iron oxides (Fig. 2), the hysteresis is related to the adsorption in the inter-particle space. The structure of synthesized pure iron oxides contains mainly mesopores, what can be seen from the distribution curve of pores (Fig. 3). The calculated micropore volume V_{micro} of investigated samples has shown that the contribution of small pores to the total pore volume is not significant.

The pore size distribution of studied samples is shown in Fig. 3, where an increase in the pore volume of composite materials A, E with regard to the natural bentonite is noticeable. Comparing the composites A and E, it can be stated that the higher pore volume was obtained for the samples A, where the content of iron oxide particles is higher. The curves for composites A are almost overlapping what means, that the temperature of synthesis had no influence on the distribution of pores. Not the same is valid for composites E: curve corresponding to the magnetic composite prepared at ambient temperature is shifted to the smaller pore diameters, what could mean that the magnetic particles precipitated on bentonite at the temperature 20 °C are smaller than those synthesized at 85 °C. The occurrence of smaller particles results in a higher surface area. The composites E20 with the highest BET surface area and the composite A85 with the highest value of total pore volume were selected for the further research.

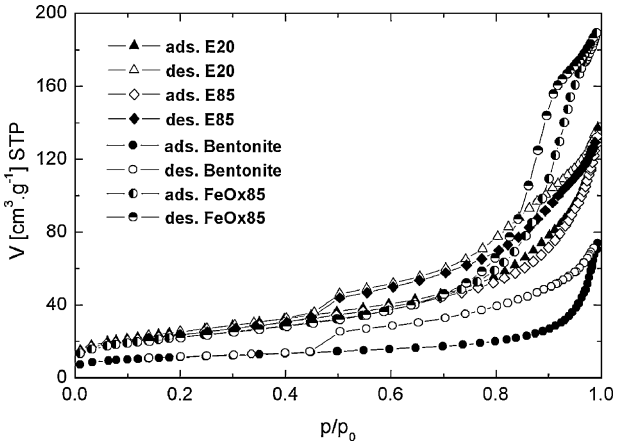

Fig. 2. N_2 adsorption/desorption isotherms of bentonite, composite E and synthetized iron oxide.

3.2. TEM analysis

TEM micrograph of the prepared composite material A85 is shown in Fig. 4. The average particle size of precipitated iron oxide particles is between 10 and 50 nm, they created the agglomerated structures non-homogenously distributed on the bentonite surface.

3.3. XRD characterization

The XRD pattern of natural bentonite is shown in Fig. 5a. The analysis confirmed the presence of monomineral montmorillonite phase. The occurrence of Fe oxidized phases was observed in both composite materials A85 and E20 (Fig. 5b and c), but it was difficult to differentiate between magnetite (Fe_3O_4) and maghemite (γ-Fe_2O_3), due to a strong overlapping of their diffraction lines [16]. According to the JCPDS PDF database, the reflections of their crystallographic planes are identical. Therefore Mössbauer spectroscopy was used for the more detailed study of iron oxide particles in the composite materials.

3.4. Mössbauer spectroscopy measurements

The room temperature Mössbauer spectrum of the composite A85 is a complex consisting of the paramagnetic doublet and one sextet (Fig. 6). The parameters obtained from the fitting by

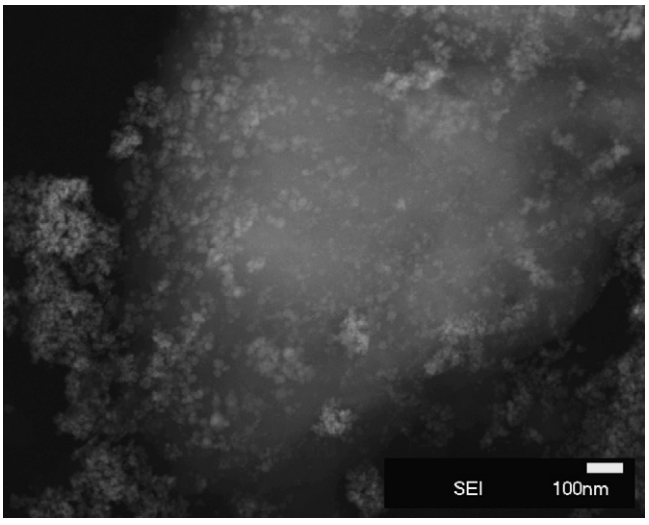

Fig. 4. FE-TEM (field emission-transmission electron microscopy) image of the composite sample A85.

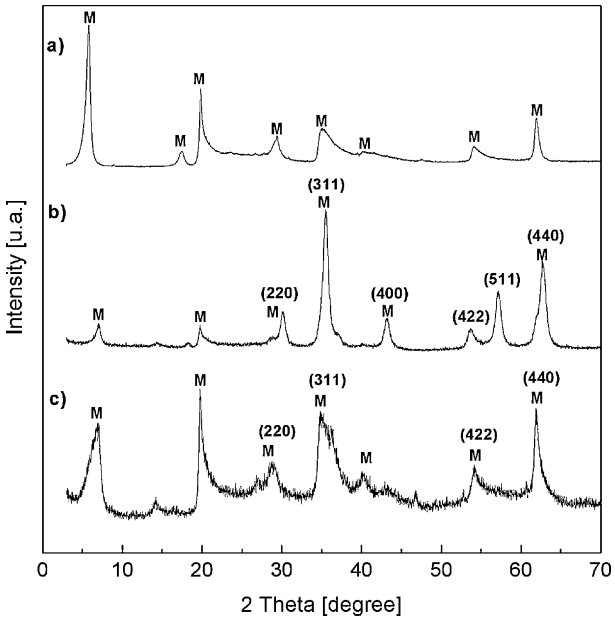

Fig. 5. XRD spectrum of (a) the natural bentonite, (b) composite sample A85 and (c) E20 (M – montmorillonite).

two sextet components show the Fe^{3+} in maghemite [17] (average hyperfine magnetic field for the octahedral site: $B^{Oct} = 38.8$ T, isomer shift IS = 0.25 mm s^{-1}, relative spectral area RA = 59.7%; for the tetrahedral site: hyperfine magnetic field $B_{hf}{}^{Tet} = 47.0$ T, IS = 0.13 mm s^{-1}, RA = 35.8%). The asymmetry in the sextet subspectra, their broadening and distribution of hyperfine magnetic fields in the octahedral position are typical for nano-meter sized particles. Two paramagnetic subspectra belong with positions of Fe^{3+} in the natural bentonite [18].

A different spectrum was detected for the composite E20, where the superparamagnetic doublet was observed (Fig. 7). The phenomena of superparamagnetism in the Mössbauer spectroscopy is connected with small magnetic particles (below 10 nm) and causes the magnetic hyperfine splitting to collaps and turn to a paramagnetic singlet or doublet. As a result, the material as a whole is not magnetized except in an externally applied magnetic field [19]. The spectrum was fitted by two components: one for the trivalent iron in bentonite and the second one also showed Fe^{3+}, for the iron oxide.

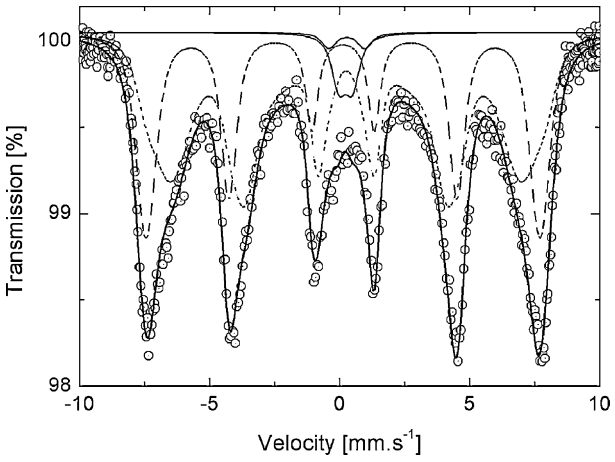

Fig. 6. Mössbauer spectrum of the composite sample A85 (long dash line belongs to the tetrahedral position of trivalent iron in maghemite, short dash line to its octahedral position, two full lines fit the paramagnetic positions of Fe^{3+} in bentonite).

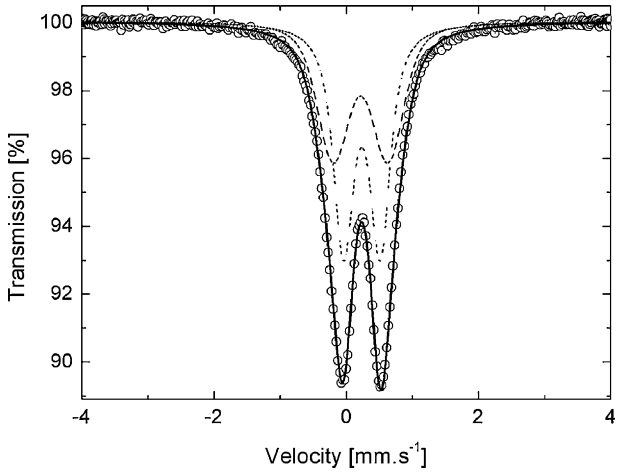

Fig. 7. Mössbauer spectrum of the composite sample E20 fitted by two superparamagnetic components (long and short dash line).

The Mössbauer analysis confirms that the present magnetic phase in the composites is maghemite and that the iron oxide particles in these composites are nano-meter sized. Also, it is pressumed from the superparamagnetic behaviour of the composite E20 that its iron oxide particles are smaller then those occurred in the composite A85, as already shown by the adsorption analysis.

3.5. ζ-Potential determinations

The ζ-potential of bentonite, iron oxide (maghemite) and their composites as a function of pH is shown in Fig. 8. We can see that the particles of natural bentonite are almost constantly negatively charged, as manifested by negative values of ζ ranging from ca. −20 to −27 mV at low and high pH, respectively. The only exception is a rather abrupt increase in the negative ζ value between pH 6 and 7. Apparently, there is no isoelectric point (IEP), as it is usual for most montmorillonites [20]. The reason is a deficiency in the positive charge due to the substitution of Al for Si in the tetrahedral sheets and Mg for Al in the octahedral sheets of the 2:1 layer of montmorillonite. The negative structural electric charge (0.66 charge per unit cell) is balanced by cations located between the unit layers of the montmorillonite dioctahedral structure. These cations are thus dissolved into the aqueous solution (leaving the surface negatively charged) and/or exchanged for other cations from the solution. There is also a pH-dependent charge on edges of the lamellar particles but it is too small to overcome the negative charge on the lamellar faces [21].

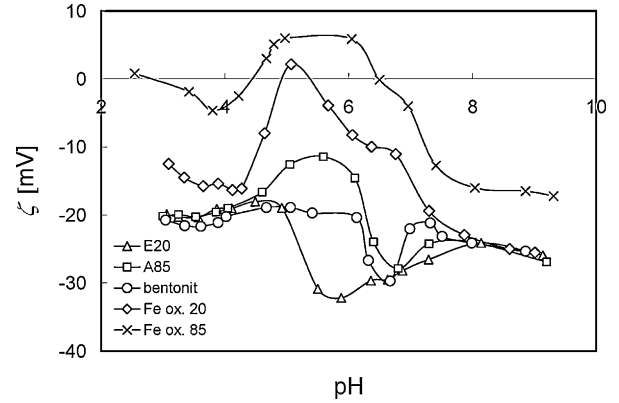

Fig. 8. ζ-vs.-pH dependence of bentonite, iron oxide and their composites.

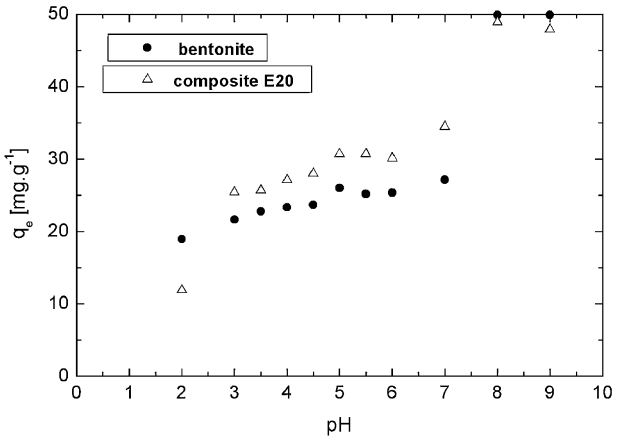

Fig. 9. Effect of solution pH on Cd^{2+} removal.

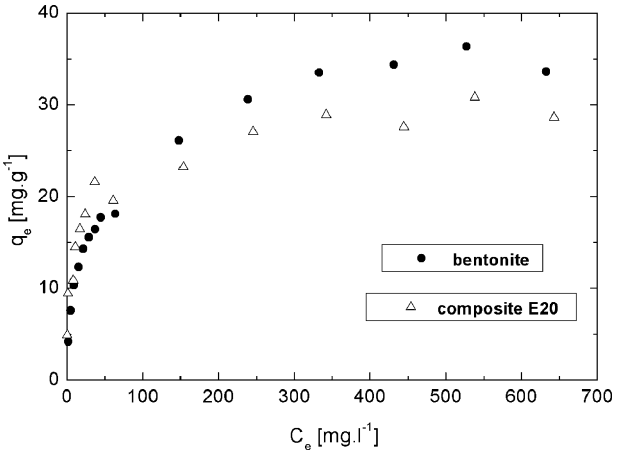

Fig. 11. Sorption of Zn^{2+} on natural bentonite and composite E20.

On the other hand, the particles of maghemite manifest two isoelectric points, at pH 4.5 and 6.5. This phenomenon is possibly connected with a low concentration of the particles in the dispersions prepared for the electrokinetic experiments. The second IEP of the maghemite sample synthesized at 85 °C, located at pH around 6.5, is however exactly the same as that published for maghemite by many authors [22–24]. Interestingly, the particles formed at the ambient temperature provide a similar but shifted ζ–pH dependence, showing a lower density of Fe functional groups on their surface.

Fig. 8 also shows that the electrokinetic response of 1:1 (A85) bentonite–maghemite composite, being characterized by a net negative charge (ζ above −10 mV) at all pHs, is intermediate between that for the unmodified bentonite and maghemite prepared at 85 °C (measured separately). This reveals that both components are exposed at the outer surface of the composite particulates. Interestingly, the ζ–pH dependence for A85 resembles that for bentonite (montmorillonite) at pH below 4.5 and above 6.5, i.e. just when the surface of maghemite and montmorillonite are equally (negatively) charged, i.e. they are electrostatically attracted. It can be expected then that the maghemite nanoparticles are desorbed from the montmorillonite sheets. That the ζ-potential of montmorillonite is only (apparently) detected in the ELS spectra of the A85 composite can be caused by the fact that the clay platelets are much bigger, providing much more intense light scattering signal, than the precipitated iron oxide nanoparticles. On the other hand, a rather firm adhesion of the positive nanoparticles can be expected on the negative montmorillonite platelets at pH from 4.5 to 6.5 due to the electrostatic attraction. Indeed, the ζ-potential course of A85 over this pH range follows that for maghemite, although with a remarkable shift towards montmorillonite, supporting the above idea of a combined maghemite/montmorillonite surface of the A85 composite particulates in the given pH range. In fact, should the maghemite be desorbed, it would not be detected in the ELS spectra.

3.6. Sorption experiments

The pH of aqueous solution is very important parameter influencing the metals sorption onto sorbent materials. To investigate the effect of solution pH on the sorption, the pH values were adjusted to the range of 2–9. The uptake of cadmium and zinc over this range of pH was studied with the initial metal concentration 100 mg/l (Figs. 9–10). It followed from the figures that the adsorption capacity of cadmium removal for all three sorbents was found stable at pH 5–6. The higher uptakes at pH above 7 are ascribed to the precipitation of hydroxides [25]. The uptake of zinc on three sorbents was found to be stable at pH 5–6. Basing on these experiments and electrokinetic studies, the sorption experiments were conducted at pH equal 5.

3.6.1. Zinc sorption

The data on Zn^{2+} sorption are shown in Figs. 11 and 12. The maximum values of the sorbed amount on bentonite and composite E20 were reached in the concentration range 10–750 mg/l (Fig. 11), while the saturated sorption on composite A85 was achieved

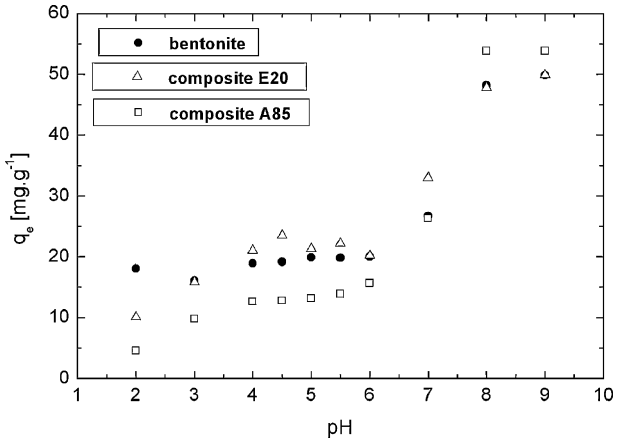

Fig. 10. Effect of solution pH on Zn^{2+} removal.

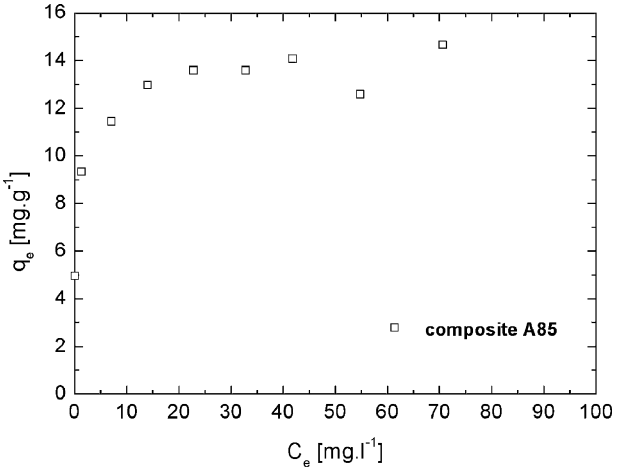

Fig. 12. Sorption of Zn^{2+} on composite A85.

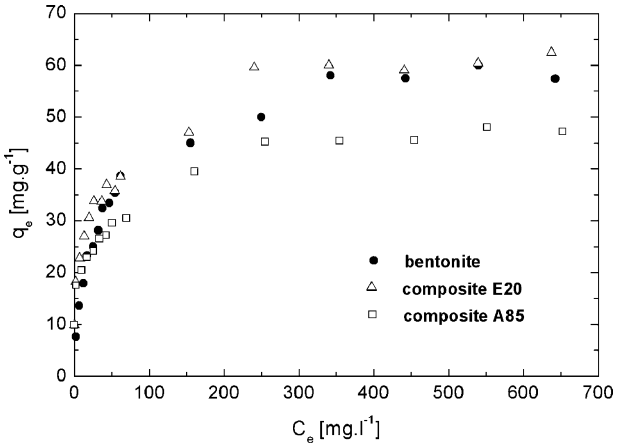

Fig. 13. Sorption of Cd^{2+} on natural bentonite, composites E20 and A85.

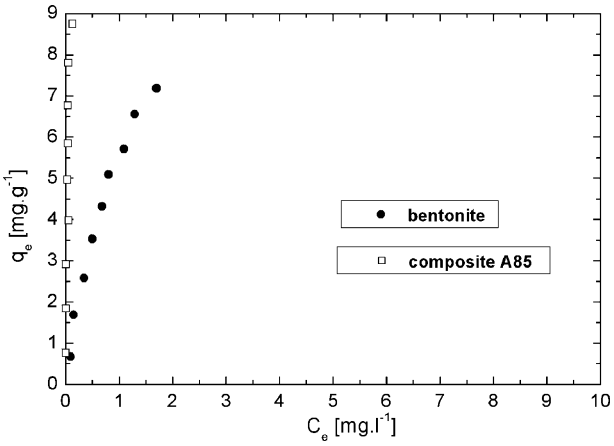

Fig. 15. Sorption of Cd^{2+} on bentonite and composite A85.

already in lower concentration range 10–100 mg/l (Fig. 12). The sorption data were well fitted to the linear form of the Langmuir isotherm:

$$\frac{C_e}{q_e} = \frac{1}{Q_m K} + \frac{C_e}{Q_m}, \quad (1)$$

where C_e is the equilibrium concentration of metal ions in the solution, q_e is the amount of metal sorbed by the adsorbent, Q_m represents the maximum adsorption capacity and K is the sorption equilibrium constant [26]. The Langmuir model parameters are presented in Table 2. The high R^2 values suggest that the Langmuir model describes the sorption data very effectively. The maximum sorption capacity for bentonite is higher than for the composites E20 and A85. However, the equilibrium values C_e obtained for composite E20 at lower concentrations of zinc ions (see Fig. 11) suggest that the sorption on composites should be favorable in the low concentration range.

3.6.2. Sorption of cadmium

The uptake of Cd^{2+} is shown in Fig. 13. The adsorption data were subjected to the Langmuir isotherm model in linear form (Eq. (1)). The calculated parameters introduced in Table 2 indicate that the composite sorbent E20 is the most suitable sorbent of Cd^{2+} in the whole initial concentration range. Additional sorption experiments were realized in concentration range 1–10 mg/l, using 1 g of sorbent (Figs. 14 and 15). These experiments confirmed that both composite sorbents E20 and A85 are more effective in Cd^{2+} sorption than the natural bentonite. The calculated sorption efficiency for both sorbents E20 and A85 was 98.7%, while for bentonite 80.9% was achieved.

3.6.3. Nickel sorption

The sorption of nickel on the sorbents is shown in Fig. 16. The plots of experimental data implied that the sorption data on bentonite and composite E20 should be tested to Freundlich isotherm model, given in its linear form:

$$\ln\ q_e = \ln K_f + n \ln C_e, \quad (2)$$

where the constants of Freundlich equation K_f and n indicate the relative sorption capacity of the adsorbent and the intensity of the adsorption. The sorption data on composite A85 were tested to Langmuir model. The results are presented in Table 3.

The values of R^2 from 0.94 to 0.98 indicate, that the sorption process is satisfactorily described by the selected isotherm models (bentonite, composite E20 – Freundlich, composite A85 – Langmuir). The constant K_f, related to the sorption capacity is higher for the composite E20. The additional sorption experiments conducted in low concentration range 1-15 mg/l (Figs. 17 and 18) showed that when using 2 g of sorbents, the efficiency could achieve 96.8% for both composites E20, A85 and 73.3% for bentonite.

The composite sorbents E20 and A85 should be very convenient for removing metals from aqueous solutions where their concentration is very low but still harmful.

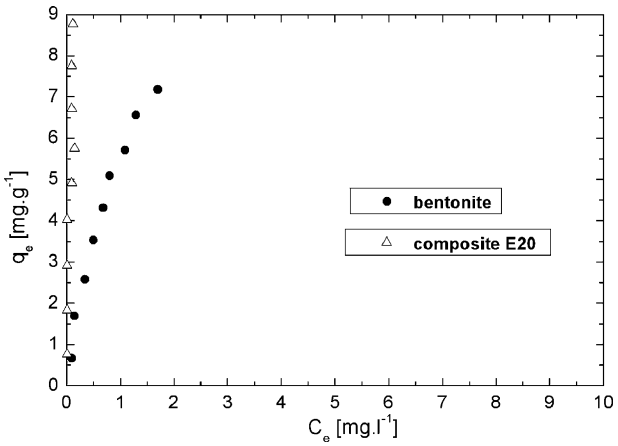

Fig. 14. Sorption of Cd^{2+} on natural bentonite and composites E20.

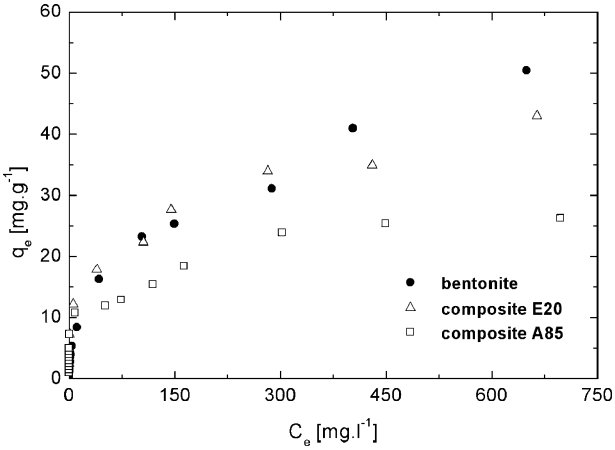

Fig. 16. Sorption of Ni^{2+} on bentonite and composites E20 and A85.

Table 2
Langmuir parameters for Zn^{2+} and Cd^{2+} sorption.

Sorbent	Zn^{2+}			Cd^{2+}		
	Q_m [mg/g]	K [l/mg]	R^2	Q_m [mg/g]	K [l/mg]	R^2
Bentonite	36.63	0.027	0.9932	61.35	0.030	0.9964
Composite E20	29.67	0.063	0.9952	63.29	0.042	0.9955
Composite A85	14.10	0.891	0.9905	48.78	0.043	0.9969

Table 3
Freundlich and Langmuir parameters for Ni^{2+} sorption.

Sorbent	Ni^{2+}					
	K_f [l/g]	n	R^2	Q_m [mg/g]	K [l/mg]	R^2
Bentonite	2.326	0.497	0.9879			
Composite E20	6.73	0.294	0.9441			
Composite A85				27.93	0.018	0.9809

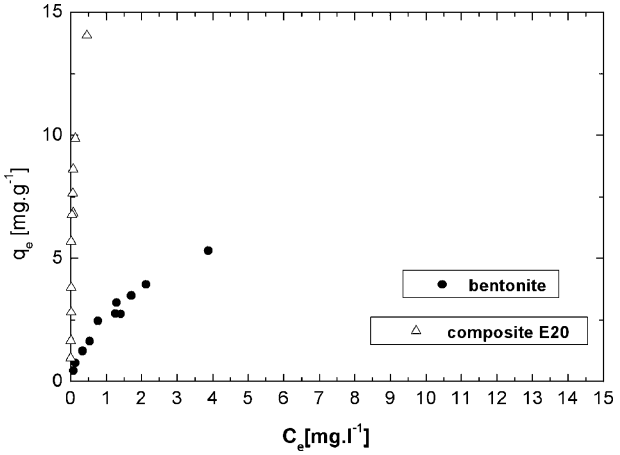

Fig. 17. Sorption of Ni^{2+} on bentonite and composite E20.

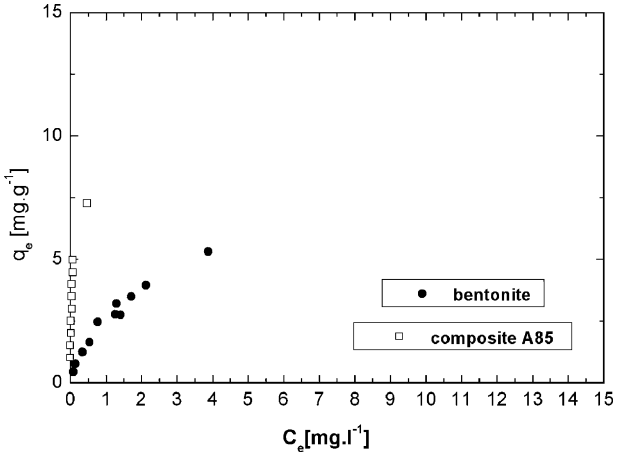

Fig. 18. Sorption of Ni^{2+} on bentonite and composite A85.

4. Conclusions

The synthesis of bentonite/iron oxides composites offered to obtain material used as sorbents of heavy metals from aqueous solutions, which due to their magnetic properties should be easily separated from the medium by applying a magnetic field. The increased specific surface area, pore volume of composites comparing to the natural bentonite suggests the formation of the agglomerated structure created from the precipitated nano-sized iron oxides on the surface of bentonite (TEM). The analysis of the composites structure explored by XRD and Mössbauer spectroscopy confirmed the maghemite phase in composites and revealed the smaller iron oxide particles in the composite E20. The composites E20 and A85 were tested for sorption of zinc, cadmium and nickel in wide initial concentration range (10–750 mg/l). Sorption experiments conducted in low concentration ranges 1–10 mg/l of cadmium and 1–15 mg/l of nickel ions showed, that the composite materials E20 and A85 possess the potentiality to be an effective sorbent for the removal of heavy metals from waters with low metal concentrations. They could be used for the purification of drinking water with a content of heavy metals exceeding the determined limits (caused by the different reasons, e.g. spates), or for the final purification of the pretreated wastewaters from the industry still containing low concentrations of unfavourable heavy metals ions.

Acknowledgements

The authors are grateful to the Slovak Scientific Grant Agency VEGA and the Research and Development Agency APVV for the financial support of the projects G/0119/29 and No. 0728-07. One of authors (Z.O.) would like to thank to DAAD (Deutscher Akademischer Austauschdienst) for the scholarship gained for a short research stay in Germany, where the XRD and Mössbauer spectroscopy measurements were done.

References

[1] S.E. Bailey, T.J. Olin, R.M. Bricka, D.D. Adrian, A review of potentially low-cost sorbents for heavy metals, Water Res. 33 (1999) 2469–2479.
[2] C. Volzone, L.B. Garrido, Retention of chromium by modified Al–bentonite, Cerâmica 48 (2002) 153–156.
[3] C.H.O. Ijagbemi, M.H. Baek, D.S. Kim, Montmorillonite surface properties and sorption characteristics for heavy metal removal from aqueous solutions, J. Hazard. Mater. 166 (2009) 538–546.
[4] S. Karahan, M. Yurdakoç, Y. Seki, K. Yurdakoç, Removal of boron from aqueous solution by clays and modified clays, J. Colloid Interface Sci. 293 (2006) 36–42.
[5] K.G. Bhattacharyya, S.G. Gupta, Adsorption of heavy metals on natural and modified kaolinite and montmorillonite: a review, Adv. Colloid Interface Sci. 140 (2008) 114–131.
[6] A. Kaya, A.H. Ören, Adsorption of zinc from aqueous solutions to bentonite, J. Hazard. Mater. B 125 (2005) 183–189.
[7] E. Eren, Removal of copper ions by modified Unye clay, Turkey, J. Hazard. Mater. 159 (2008) 235–244.
[8] L. Oliveira, R.V.R.A. Rios, J.D. Fabris, K. Sapag, V.K. Garg, R.M. Lago, Clay–iron oxide magnetic composite for the adsorption of contaminants in water, Appl. Clay Sci. 22 (2003) 169–177.
[9] Š. Jakabský, M. Lovás, F. Blaško, Use of Ferromagnetic Fluids in the Mineral Processing, Grafotlač, Košice, 2004.
[10] P. Yuan, M. Fan, D. Yang, H. He, D. Liu, A. Yuan, J.X. Zhu, T. Chen, Montmorillonite-supported nanoparticles for the removal of hexavalent chromium [Cr(VI)] from aqueous solutions, J. Hazard. Mater. 166 (2009) 821–829.
[11] X. Peng, Z. Luan, H. Zhang, Montmorillonite–Cu(II)/Fe(III) oxides magnetic material as adsorbent for removal of humic acid and its thermal regeneration, Chemosphere 63 (2006) 300–306.

[12] K. Kluchova, R. Zboril, J. Tucek, M. Pecova, L. Zajoncova, I. Šafarik, M. Mashlan, I. Markova, D. Jancik, M. Sebela, H. Bartonkova, V. Bellesi, P. Novak, D. Petridis, Superparamagnetic maghemite nanoparticles from solid-state synthesis—their functionalization towards peroral MRI contrast agent and magnetic carrier for trypsin immobilization, Biomaterials 30 (2009) 2855–2863.
[13] K. Jesenák, V. Hlavatý, Laboratory device for sedimentation of fine bentonite fractions, Scripta Fac. Sci. Nat. Univ. Masarik. Brun. Geol. 28–29 (2000) 33–36.
[14] K. Lagarec, D.G. Rancourt, Recoil—Mössbauer Spectral Analysis Software for Windows, Version 1.02, Department of Physics, University of Ottawa, Canada, 1998.
[15] K.S.W. Sing, D.H. Everett, R.A.W. Haul, L. Moscou, R.A. Pierotti, J. Rouquérol, T. Siemieniewska, Reporting physisorption data for gas/solid systems, Pure Appl. Chem. 57 (1985) 603–619.
[16] R.E. Vandenberghe, C.A. Bariero, G.M. da Costa, E. Van San, E. De Grave, Mössbauer characterization of iron oxides, Hyperfine Interact. 126 (2000) 247–259.
[17] Ö. Helgason, J.M. Greneche, F.J. Berry, S. Morup, F. Mosselmans, Tin- and titanium-doped γ-Fe_2O_3 (maghemite), J. Phys. Condens. Matter 13 (2001) 10785–10797.
[18] E. Murad, J.H. Johnston, Iron oxides and oxyhydroxides Mössbauer Spectroscopy Applied to Inorganic Chemistry, vol. 2, Plenum Press, New York, London, 1987, pp. 507–582.
[19] T. Szabó, A. Bakandritsos, V. Tzitzios, S. Papp, L. Kőrösi, G. Galbács, K. Musabekov, D. Bolatova, D. Petridis, I. Dékány, Magnetic iron oxide/clay composites: effect of the layer silicate support on the microstructure and phase formation of magnetic nanoparticles, Nanotechnology 18 (2007) 285602–285610.
[20] M.S. Celik, Electrokinetic behaviour of clay surfaces, in: F. Wypych, K.G. Satyanarayana (Eds.), Clay Surfaces. Fundamentals and Applications, Interface Science and Technology Series, vol. 1, Elsevier Ltd., Amsterdam, 2004, pp. 57–89.
[21] G.A. Parks, The isoelectric points of solid oxides, solid hydroxides, and aqueous hydroxo complex systems, Chem. Rev. 65 (1965) 177–198.
[22] M. Kosmulski, Surface Charging and Points of Zero Charge, Surfactant Science Series, First ed., CRC Press, 2003.
[23] H. Watanabe, J. Seto, The catalysis of maghemite and hematite on the aldol and the retro-aldol condensation of acetone, Bull. Chem. Soc. Jpn. 64 (1991) 2411–2415.
[24] C.J. Serna, M.P. Morales, Maghemite (γ-Fe_2O_3): a versatile magnetic colloidal material, in: E. Matijevic, M. Borkovec (Eds.), Surface and Colloid Science, vol. 17, Kluwer Academic/Plenum Publishers, New York, 2004, pp. 27–81.
[25] A. Özer, H.B. Pirinççi, The adsorption of Cd(II) ions on sulphuric acid-treated wheat bran, J. Hazard. Mater. B 137 (2006) 849–855.
[26] Y.S. Ho, W.T. CHiu, Ch.Ch. Wang, Regression analysis for the sorption isotherms of basic dyes on sugarcane dust, Bioresour. Technol. 96 (2005) 1285–1291.